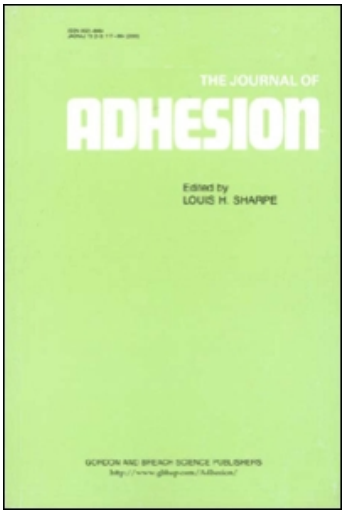

The Journal of Adhesion
Publication details, including instructions for authors and subscription information:
http://www.informaworld.com/smpp/title~content=t713453635

Fracture Toughness of Adhesive Joints

S. Mostovoy[a]; E. J. Ripling[a]; C. F. Bersch[b]
[a] Materials Research Laboratory, Inc., Glenwood, Illinois, U.S.A. [b] Naval Air Systems Command, Washington, D.C., U.S.A.

To cite this Article Mostovoy, S. , Ripling, E. J. and Bersch, C. F.(1971) 'Fracture Toughness of Adhesive Joints', The Journal of Adhesion, 3: 2, 125 — 144
To link to this Article: DOI: 10.1080/00218467108081159
URL: http://dx.doi.org/10.1080/00218467108081159

J. Adhesion, 1971, Vol. 3, pp. 125–144

Printed in Northern Ireland

Fracture Toughness of Adhesive Joints†

S. MOSTOVOY, E. J. RIPLING

Materials Research Laboratory, Inc., Glenwood, Illinois, U.S.A.

C. F. BERSCH

Naval Air Systems Command, Washington, D.C., U.S.A.

(*Received November* 24, 1970)

To define the influence of the processing variables on the resistance of epoxy joints to brittle crack extension during short loading times, the fracture toughness, $\mathcal{G}_{IC}$, of the joints was measured as a function of the following variables:

1. Hardener type (TEPA vs. HHPA)
2. Ratio of hardener to resin content
3. Post-cure temperature

and 4. Joint geometry (thickness and width)

It was found that the toughness of the TEPA hardened system varied by a factor of four-to-one as the ratio of hardener to resin content and post-cure temperature varied within what might be considered reasonable limits for manufacturing. The toughness of the HHPA hardened system varied only over the middle half of this same range.

For both systems, toughness increased with joint thickness over the range of 2 to 50 mils.

INTRODUCTION

The design of structures incorporating adhesively joined components has always been more difficult than that involving monolithic materials because of the complex and generally unanalyzable state of stress present in the adhesive joint. In addition, structural design using monolithic materials has been based on yield stress with safety factors selected on the basis of

†First presented at the 2nd National SAMPE Technical Conference; Dallas, Texas, October 6–8, 1970; copies of the reprint book may be purchased for $30 from SAMPE National Business Office, Azusa, California 91702.

toughness tests. Since bonded joints always fail by progressive crack extension, no gross or average stress criteria are adequate to describe their structural performance. Therefore, the strength of the bonded structure is controlled by the presence of flaws inherent in the manufacture of the adhesive joints, i.e., bubbles, dust particles and unbonded or poorly bonded areas. Accordingly, designs must be based on a fracture criterion.

Monolithic materials for structures have substantial flaw tolerance; bonded materials have little flaw tolerance. The joining of high modulus materials with a low modulus adhesive localizes the deformation, associated with loading, to the area of the low modulus adhesive and results in high local strains and subsequent crack extension from pre-existing flaws. Since this phenomenon occurs as a result of geometry, the bulk properties of the adhesive are of less importance than the fracturing behavior of the material with similar geometric constraints imposed.

The techniques of fracture mechanics developed by G. R. Irwin[1] make it possible to measure the energy lost to a growing crack, if a suitable specimen analysis can be made. A well characterized specimen has been developed by the authors for application of fracture mechanics to opening mode loading[2-5]. This specimen, used for the evaluation of adhesive joints, and shown in Figure 1, makes use of a large flaw which overrides the small naturally present manufacturing defects. Ordinarily, calculations of the energy lost to a growing crack require a simultaneous knowledge of two related parameters, i.e., the load and the crack length, to determine adhesive fracture toughness, $\mathcal{G}_{IC}$. This particular specimen, however, has been designed such that only load need be known to determine $\mathcal{G}_{IC}$. The expression that relates applied crack extension force, $\mathcal{G}$, with applied load, P, and crack length, a, is[4]:

$$\mathcal{G} = \frac{P^2}{2b}\frac{\partial C}{\partial a}$$

where b is the specimen width and C the system compliance (i.e., displacement divided by load) for a given crack length a. The crack-length-independent expression for opening mode loading, which results in crack extension normal to the applied load, is:

$$\mathcal{G}_i = \frac{P_i^2}{2b}\frac{8}{Eb}m$$

where P is the instantaneous load and m is a constant, having dimension of in.$^{-1}$, determined by adherend manufacture, viz.:

$$m = \left(\frac{3a^2}{h^3} + \frac{1}{h}\right)$$

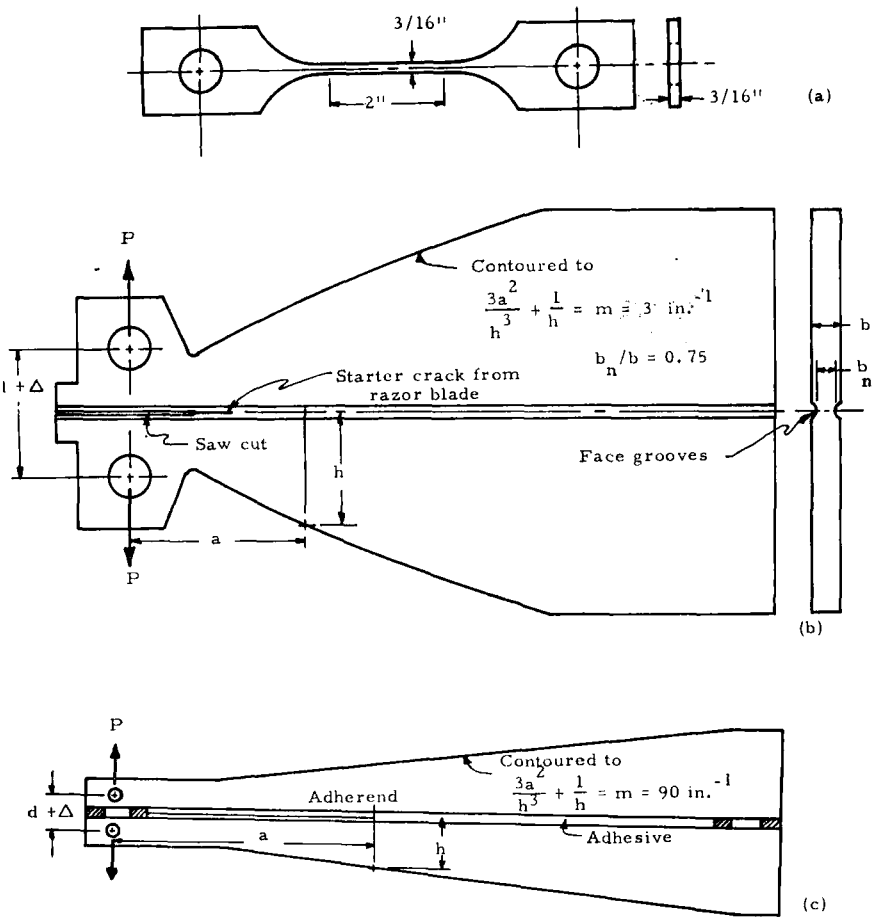

FIGURE 1. Schematic diagrams: (a) tensile specimen; (b) Tapered double cantilever-beam specimen (m = 3) (bulk specimen); (c) Tapered double cantilever-beam specimen (m = 90) (joint specimen).

For large values of m the expression for $\mathcal{G}$ is exact, i.e., $m = 90$ in.$^{-1}$. However, at m values approaching 1 in.$^{-1}$, corrections made using calibration techniques must be applied that alter the calculated m value as much as 30 percent.

A load displacement record of an adhesive joint test shows that at crack lengths where the specimen is valid, an instability point is reached where a stationary crack begins to move. The critical load value associated with this instability is used to calculate the critical crack extension force $\mathcal{G}_{IC}$, using the equation given above. While the opening mode loading condition is deemed most serious, the general expression for $\mathcal{G}$ enables us to determine

the critical crack extension force in either of the other (e.g., shear) modes of loading. The mathematics that describe the relation between specimen geometry and the extension of fracture mechanics to the two shear modes have been described earlier[8].

MATERIALS AND TEST PROCEDURE

The critical crack extension force or fracture toughness, $\mathcal{G}_{IC}$, of a number of adhesive materials has been determined, using the tapered double cantilever beam specimen (TDCB) described. A well characterized resin system with two hardening agents has provided the base materials for developing test techniques.

The commercial resin DER 332 was the basis for two adhesive formulations using a low temperature curing amine hardener (TEPA) and an elevated temperature curing anhydride (HHPA). Manufacturing variables, i.e., composition and post-cure temperatures, joint geometry and surface finish, were varied to determine the effect of each of these on the resistance of the material to the propagation of a natural crack. In addition, tensile properties were determined for each composition and post-cure temperature used in the fracture study. The adhesive materials used in the test program were evaluated as monolithic materials and as adhesive joints with a variety of thicknesses. The standard thickness selected for the bulk of the study was 0.005 inch (5 mils) since it was determined that small errors in thickness at this value did not influence the measured toughness.

Tensile properties were measured with specimens of the type shown in Figure 1-a. The toughness of bulk materials was measured with linear compliance specimens (TDCB) of a contour corresponding to an m value of 3 in.$^{-1}$, Figure 1-b. Bond toughness was measured primarily with $\frac{1}{2}$ inch thick aluminum adherends having a 25 μ in. bond surface finish; however, steel and glass adherends were found to yield identical values of $\mathcal{G}_{IC}$ when bonded with adhesive of the same formulation and post-cure. The surface finish on glass adherends ranged from 1 to 50 μ in., and that of steel between 3 and 200 μ in. Aluminum adherends have been made from 15 to 50 μ in. with no effect on $\mathcal{G}_{IC}$. Aluminum adherends were machined into an $m = 90$ in.$^{-1}$ contour, Figure 1-c, and cleaned with the standard hot sulfuric acid-chromic acid-water solution. For low viscosity relatively fluid adhesive systems, specimen manufacture began with placing the dried adherends together, bond sides facing, and screwing them together on each end. A pair of 5 mil shims on either side of each screw provided the separation for the bond thickness. All handling of the adherends is done by clean tongs,

tweezers and screwdriver by a gloved technician. Once screwed together the entire unit is Teflon-taped, leaving a casting dam surrounding the 10 inch long 5 mil wide gap. In addition, a one inch long strip of tape is placed in the bond near the loading holes for a crack starter and to prevent the leakage of adhesive during casting. The taped specimen is then placed on a hot plate and heated to approximately 150°F. Once the specimen has come to temperature, the hardener is thoroughly mixed with heated resin for about a minute. This fluid mixture is then slowly poured into the mold cavity starting from one end to allow air in the gap to escape. Excess adhesive is removed by trowelling with a glass rod before gelation, which occurs between 15 minutes and one hour. Because of the tape placement, the overrun occurs on only one of the four adherend faces.

This procedure was followed for the room-temperature-curing amine system, but was modified slightly for the higher temperature anhydride cured systems, viz.: the temperature of the resin is somewhat higher, the hardener is also heated prior to mixing, and an accelerator is used.

Testing of all specimens was done in a commercial screw driven tensile machine. Tensile test specimens were pulled at a crosshead rate of 0.05 in/min., while toughness test rates were varied from this slow rate to more than 50 in/min. Load-displacement records for all low to moderate rate tests were obtained either on an X-Y plotter or, for rapid tests, on an oscilloscope. The tensile extensometer was a standard friction-clamp, 2 inch gage length, 0.10 inch total extension unit which was adequate to determine the entire P-Δ curve for these relatively brittle plastics. For toughness tests where $\mathcal{G}$ is independent of crack length, either crosshead displacement or specimen opening was plotted against the load obtained as the output from a standard load cell.

For reasons to be discussed later in the paper, three particular adhesive systems were selected for detailed study after a tensile and toughness survey of the range of possible manufacturing variables. Using DER 332 as the base resin, the three were, 10 PHR of TEPA post-cured at 180°F (10T/180†), 12.5 PHR of TEPA post-cured at 270°F (12.5T/270) and 70 PHR of HHPA post-cured at 311°F (70H/311).

TENSILE PROPERTIES OF BULK ADHESIVE

Tensile property data for the TEPA hardened epoxy are shown in Figure 2 and for the HHPA cured material in Figure 3. A property comparison

† Adhesives are identified as follows:
First number = PHR of hardener
Letter = hardener, T = TEPA and H = HHPA
Second number = post-cure temperature in °F for five hours.

between the two materials, while somewhat obscured by scatter inherent in the testing of low elongation materials, reveals that, above stoichiometry, increases in hardener content result in opposite effects. For the TEPA cured resin, Young's modulus, E, decreases and elongation increases, while the opposite is true for the HHPA adhesive. As hardener content is decreased below stoichiometry there is less change in modulus, both systems showing some increase. Tensile strength and elongation increase or remain constant with hardener content for TEPA epoxy, but decrease for HHPA cured resin. Yield strength curves, defined by one percent total offset for both materials, follow the shape of the elastic modulus data. This shape can be seen more

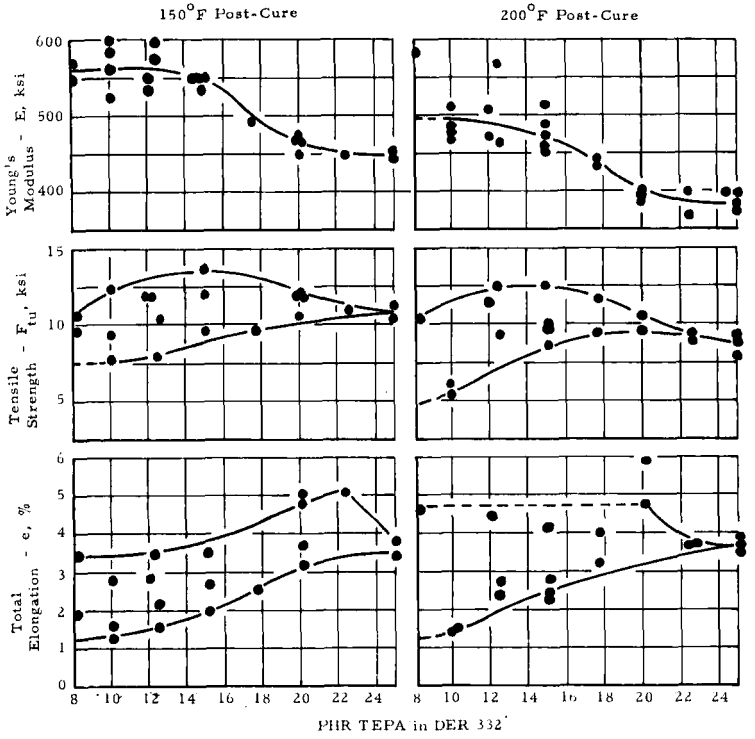

FIGURE 2 Tensile properties of epoxy as a function of composition for two post-cure temperatures. Specimen cross section $\frac{1}{8}$ x $\frac{3}{8}$ in. on a 2-in. gage length; post-cure time 5 hr.

easily in a plot of E vs. post-cure temperature shown for both materials in Figure 4. For the TEPA cured system, increases in either post-cure temperature or hardener content result in decreases in E. For HHPA cured resin,

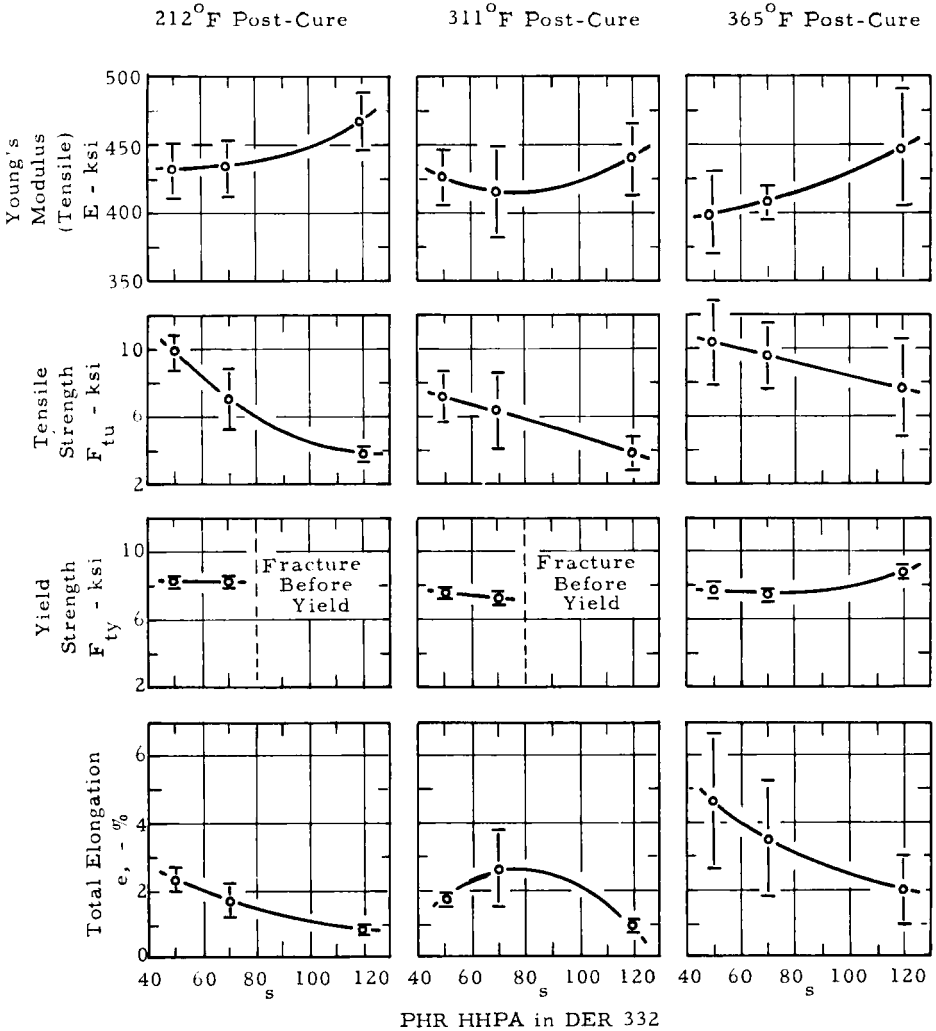

FIGURE 3 Mechanical properties of bulk epoxy as a function of composition for three post-cure temperatures. Post-cure time, 5 hrs.

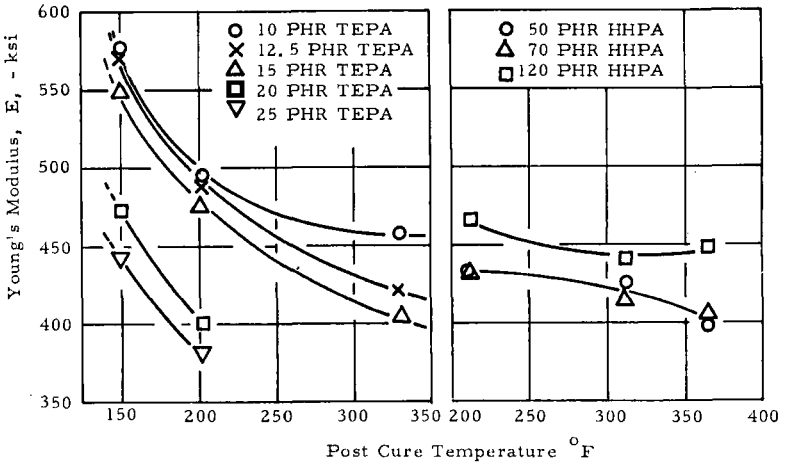

FIGURE 4 Young's modulus of bulk epoxy as a function of post-cure temperature with composition as a parameter. Left curve: TEPA cured DER 332. Right curve: HHPA cured DER 332.

there is less total change in E when the post-cure temperature of this material is increased, however, the trend is toward decreases in E with increases in post-cure temperature as with the TEPA cured system.

TOUGHNESS OF BULK EPOXY AS A FUNCTION OF COMPOSITION AND POST-CURE TEMPERATURE

Measurement of $\mathcal{G}_{IC}$, using the specimen shown in Figure 1-b, were performed on both TEPA and HHPA cured epoxy. The data obtained are

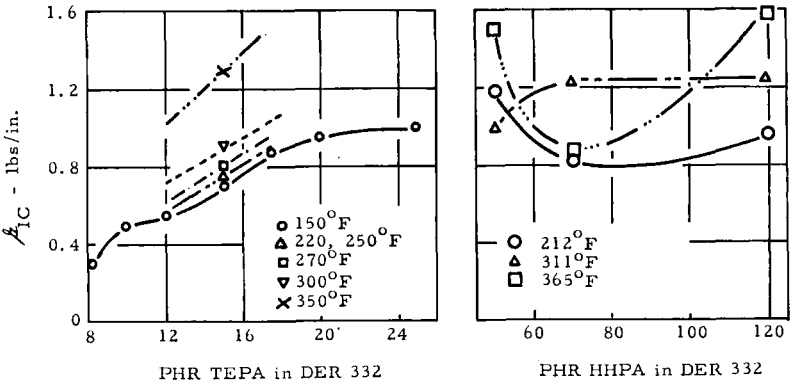

FIGURE 5 Bulk toughness as a function of composition with post-cure temperature as a parameter. Left: TEPA cured. Right: HHPA cured.

shown in Figure 5. For TEPA cured material, increases in either post-cure temperature or hardener content resulted in increased toughness, which resembled the inverse of the curves developed for E as a function of these manufacturing variables. For the HHPA cured resin there was less change in toughness with either of these variables, however, increases in post-cure temperature did tend to result in higher toughnesses where increases in hardener content did not. This HHPA hardener data, coupled with the greater scatter in properties, also was similar to the inverse of tensile modulus results with change in composition and cure temperature.

TOUGHNESS OF ADHESIVE BONDS

Effect of Composition and Post-Cure Temperature

Determination of bond toughness, $\mathcal{G}_{IC}$, was made with the $m = 90$ in.$^{-1}$ specimen shown in Fig. 1-c. For the TEPA cured resin, an extensive survey was made of the effect of manufacturing variables, i.e., hardener content, post-cure temperature, surface finish and bond-thickness on $\mathcal{G}_{IC}$. In addition, the effect of crosshead rate on toughness for 5 mil thick bonds was deter-

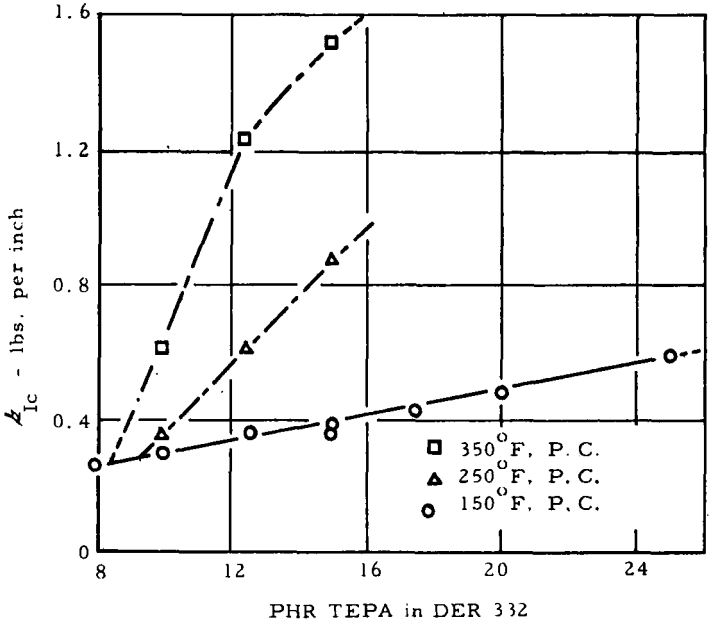

FIGURE 6 Joint toughness as a function of composition for three post-cure temperatures for TEPA system (post-cure time, 5 hrs.). Ref. 4.

mined for a number of adhesive compositions and post-cure temperatures. Both hardener content and post-cure temperature were varied over wide limits, Figure 6; and for this adhesive, at a bond thickness of 5 mils, increases in either of these variables caused increases in toughness and as much as 4 to 1 difference in resistance to the propagation of a brittle crack, i.e., $\mathcal{G}_{IC}$, was observed. In addition to the differences in $\mathcal{G}_{IC}$ there were two other changes in cracking behavior. First, at either high hardener contents (above stoichiometry) and/or high post-cure temperatures, failure location tended to shift from cohesively at the center of the bond (CoB) to adhesively at the interface (IF). Second, the cracking rate sensitivity increased with increases in these variables. In a toughness test where a rising-load is applied on the crackline, specimen geometry dictates that a crack once started cannot completely separate the two adherends without an intermediate arrest, i.e., there is a continuously decreasing energy available to a growing crack. The degree of rate sensitivity can be defined by the jump length of an initially stationary crack. Thus, an adhesive material which exhibited a small jump-length, i.e. 0.10 inches, would be less rate sensitive than one where the crack jumped an inch or more. In a load-displacement, P-Δ, record, the rate sensitive material would show a "peaked" behavior (Figure 7-a), i.e., a large difference between the load associated with $\mathcal{G}_{IC}$ and the load at which a moving crack will be arrested by the material, $\mathcal{G}_{IA}$. For a rate insensitive material, there will be little difference between $\mathcal{G}_{IC}$ and $\mathcal{G}_{IA}$, hence its P-Δ record will be "flat", Figure 7-b. Both the differences in toughness and in cracking behavior that result from changing compositional and post-cure variables suggested that two particular adhesive materials be used to evaluate the effect of other service variables such as bond thickness, loading rate sensitivity and resistance to stress corrosion cracking. The two materials selected, as noted earlier, were 10T/180, as an example of a rate insensitive, low toughness epoxy, and 12.5T/270, which represented a material having high toughness and high rate sensitivity.

Bond toughness of HHPA cured resin was considerably less sensitive to changes in either composition or post-cure temperature. As with the TEPA cured resin, this behavior is inverse to the change in tensile modulus (or yield strength). This material showed about the same rate sensitivity ($\mathcal{G}_{IC} - \mathcal{G}_{IA} \cong 0.1$ lbs/in.) over the entire range of composition and cure temperature limits used. Toughness varied from 0.72 to 0.45 lbs/in., Figure 8, or less than 2: 1, compared to more than 4: 1 for the amine hardened epoxy. Because of these small differences, a less-than-stoichiometric resin post-cured at an intermediate temperature, i.e., 70H/311, was used for evaluation of $\mathcal{G}_{IC}$ as a function of other variables such as bond thickness, discussed in this paper, and stress corrosion cracking, discussed in Ref. 9.

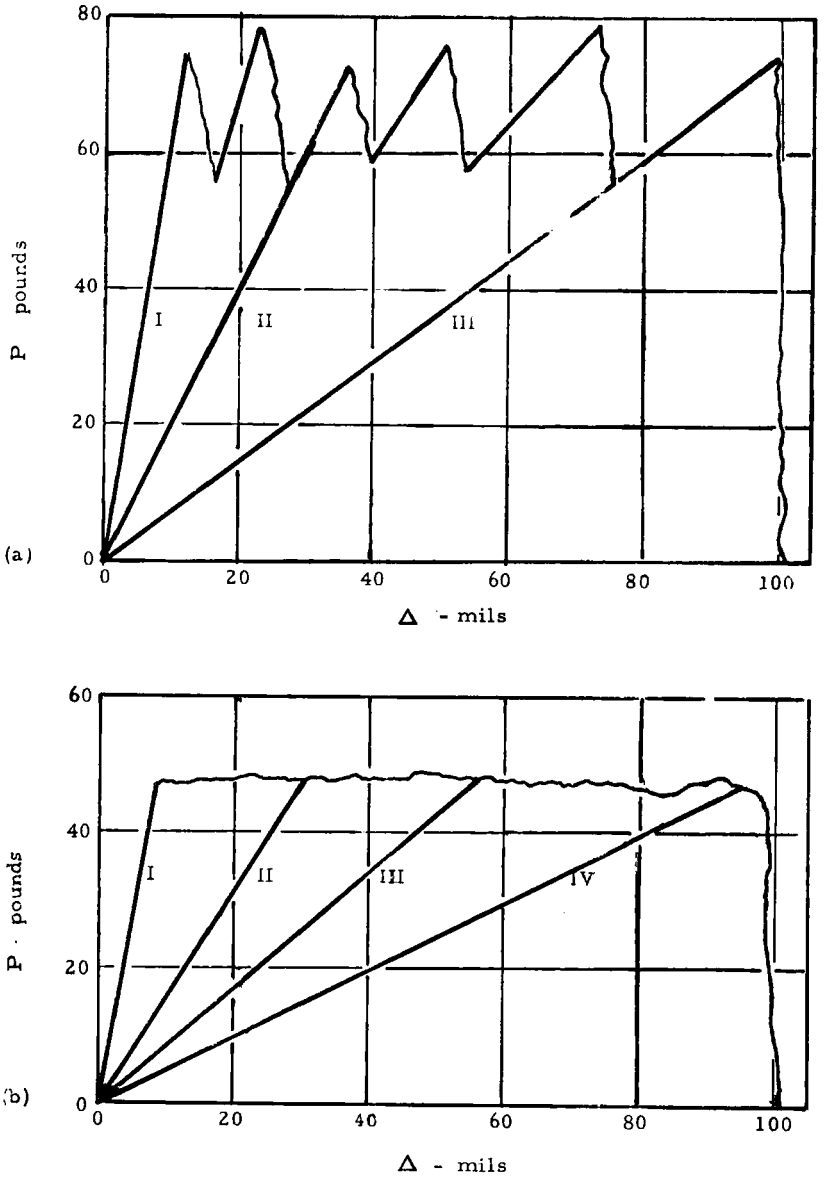

FIGURE 7. Two types of P-Δ curves. (a) Unstable ("peaked") behavior. (b) Stable ("flat") behavior. Numbers on diagrams indicate unloading and reloading lines.

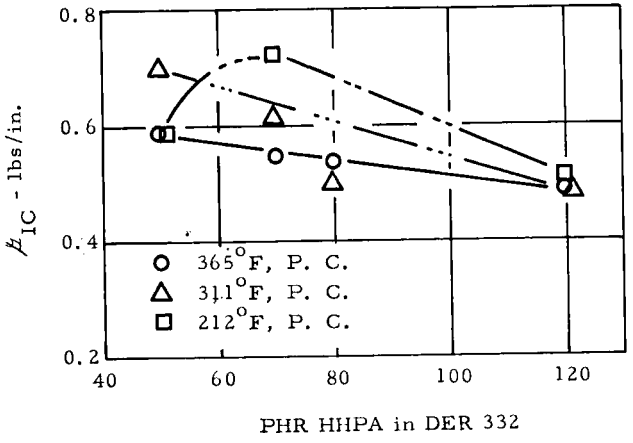

FIGURE 8. Joint toughness of HHPA cured DER 332 as a function of composition for three post-cure temperatures.

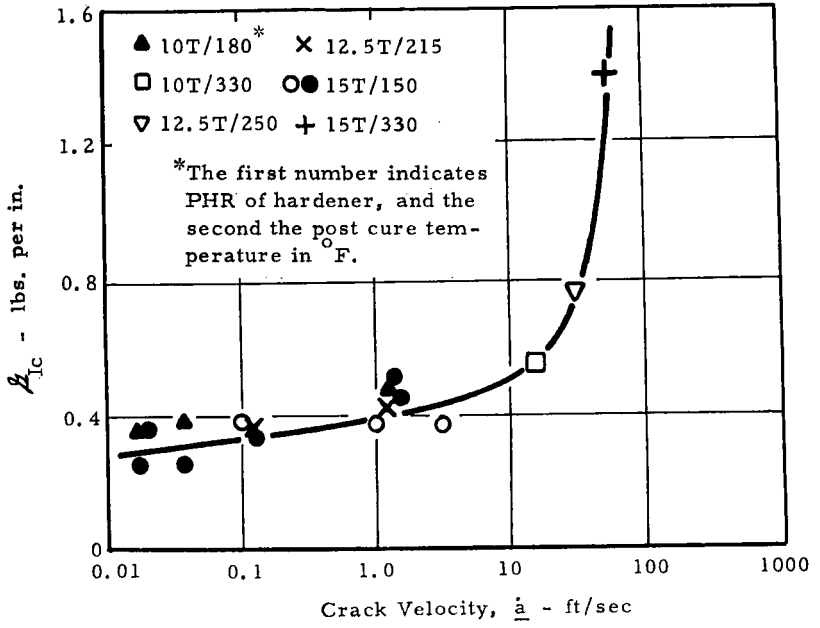

FIGURE 9 Dependence of toughness on crack velocity. Ref. 4.

EFFECT OF RATE

The effect of cracking velocity on toughness was measured on a number of different TEPA cured DER 332 systems, Figure 9, with the result that high crack velocity was associated with high toughness and rate sensitivity. Measurements of crack velocity were made using a 100 Hz. oscillator to mark the running crack, which, although somewhat inaccurate at the higher velocities, indicated that at toughness above 1.2 lbs/in. the crack velocity was of the order of 100 ft/sec. Attempts have been made to drive the crack faster than this velocity. However, experimental details have allowed the attainment of approximately 100 ft/sec., but no higher. When driven at these high cracking rates the P-Δ curve indicates the same $\mathcal{G}_{IC}$ as at low crosshead rates, but the "peaked" appearance becomes "flat" as for the low-rate-sensitive materials. At higher rates than those already attained, the crack would be driven so that the P-Δ curves would be expected to remain flat but $\mathcal{G}_{IC}$ should increase. For the low-rate-sensitive materials, where the cracking rate is essentially dictated by the crosshead rate, increases in cracking rate still result in flat P-Δ curves but higher toughness levels.

EFFECT OF BOND THICKNESS

When the bond thickness of 10T/180 was increased there was a general increase in $\mathcal{G}_{IC}$ scatter; however, $\mathcal{G}_{IC}$ did increase above 10 mils to a maximum at 50 mils, Figure 10. In addition, somewhat "peaked" P-Δ curves indicated increased rate sensitivity, accompanied by an undulating rougher fracture surface, Figure 11. At thicknesses above 50 mils, rising-load cracking tended to occur near the interface (IF) at decreasing toughnesses that approached zero as thickness approached 200 mils. Increases in specimen width from $\frac{1}{2}$ to three inches at a constant bond thickness of 50 mils did not change the basic fracturing pattern or $\mathcal{G}_{IC}$ value. Changing the specimen configuration to a taller pair of beams, i.e., $m = 4$ from $m = 90$, Figure 12, also did not change either the fracture morphology or toughness of the 50 mil bond at low cracking rates. The $m = 4$ specimen allowed testing at higher cracking rates which did, however, change the fracture morphology from rough and undulating to smooth and "frosted" (compared to smooth and shiny for thin bonds). Toughness at this higher rate was of the order of 0.30 lbs/in., which compares to thin bonds.

For 12.5T/270 adhesive, $\mathcal{G}_{IC}$ also increased with bond thickness reaching a maximum at 25 mils and decreasing thereafter. This rate sensitive adhesive

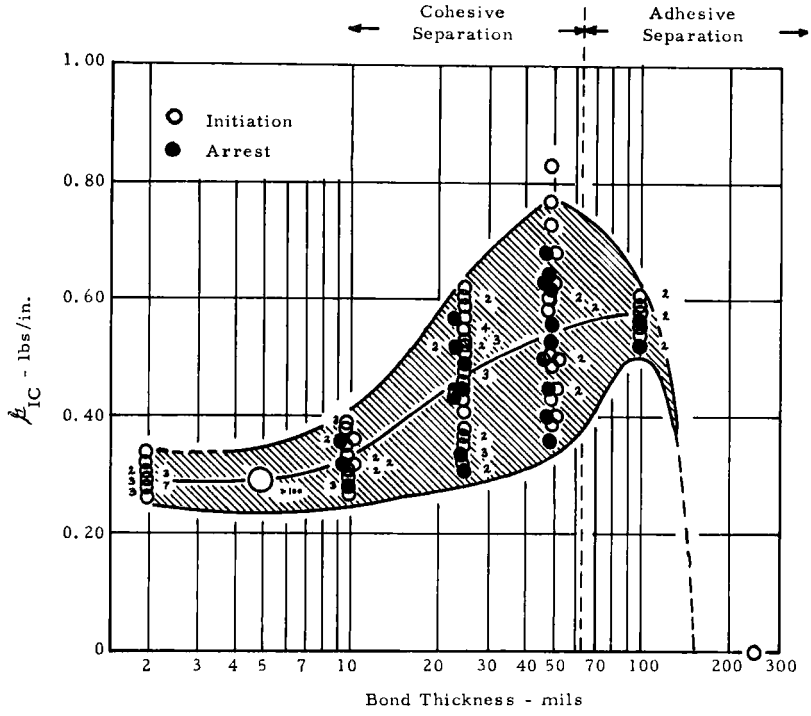

FIGURE 10 Effect of joint thickness on the toughness of 10T/180 adhesive. Cross hatched area represents 2σ limits, and solid curve is mean. (Number in parentheses represent number of tests associated with each data point. Unmarked points are single values.) Ref. 7.

showed considerable scatter in $\mathcal{G}_{IC}$ at the 5 mil thickness ($\mathcal{G}_{IC}$ = 0.65 lbs/in.; 2σ range 0.38 to 0.90 lbs/in.) and this inherent scatter became very broad for the 25 mil bonds ($\mathcal{G}_{IC}$ = 1.08 lbs/in.; 2σ range 0.58 to 1.48 lbs/in.). Beyond 25 mils, $\mathcal{G}_{IC}$ decreased and above 50 mils separation tended to be IF. Toughness decreased to zero at about 200 mils. Fracture morphology as a function of joint thickness was similar to that shown for 10T/180.

The anhydride hardened epoxy had less scatter than either of the amine cured systems and showed a continued increase in cohesive $\mathcal{G}_{IC}$ as bond thickness increased, Figure 13. Toughness at 5 mils was 0.65 lbs/in. compared to 1.9 lbs/in. at 250 mils. Above 100 mils, however, there was a tendency for interface failure. Again, thick bond fracture appearance was similar to that observed on the amine systems.

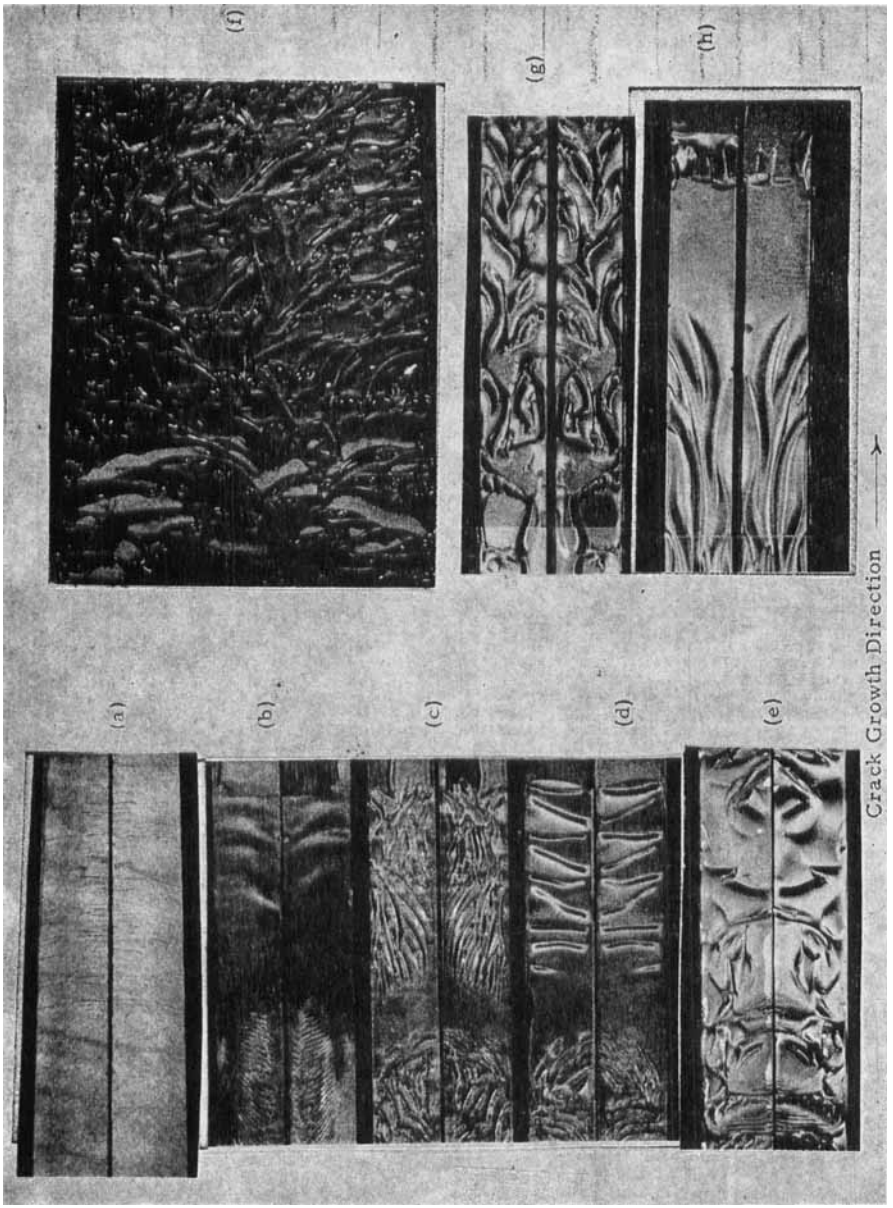

FIGURE 11 Fracture morphology of 10/180 adhesive joints from 10 to 50 mils thickness. (a) 5 mil; (b) 10 mil; (c) and (d) 25 mil; (e) 50 mil; [(a) through (e) half inch wide specimens] (f) 50 mil three inch wide specimen. (g) and (h) 50 mil (m = 4). Note: Photo (a) taken using specular reflection to reveal micro-ripple pattern. Ref. 7.

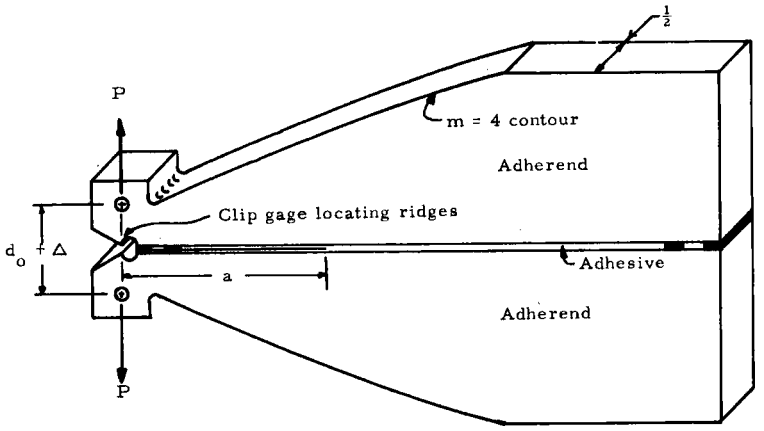

FIGURE 12 Contoured double cantilever beam adhesive specimen for high strain rate studies (m = 4).

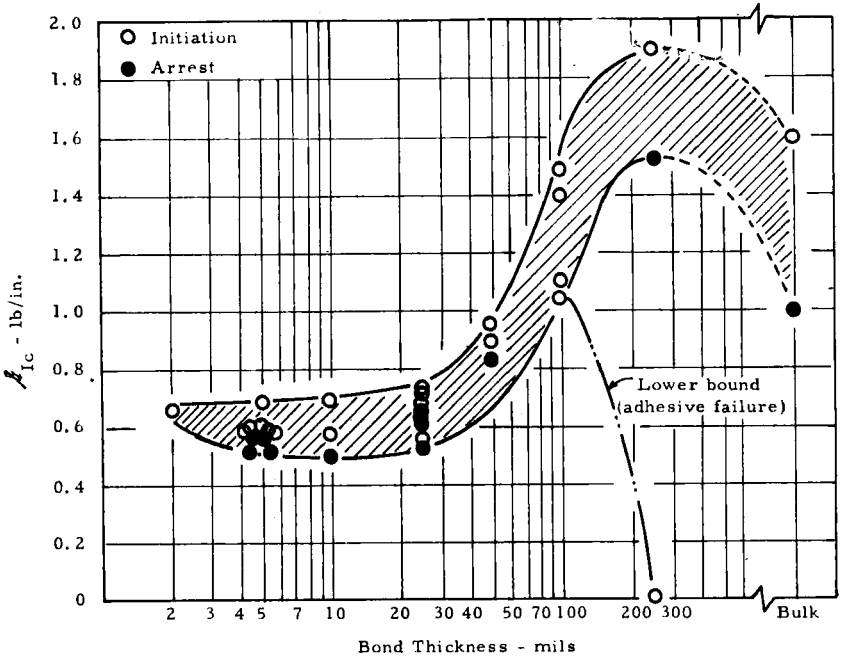

FIGURE 13 Effect of joint thickness on the toughness of 70H/311 adhesive. All fractures cohesive except lower bound line.

COMPARISON OF BULK AND BOND TOUGHNESS

Bulk and bond toughness for the systems studied are not simply related. As was stated earlier for TEPA cured resin, increasing toughness was observed

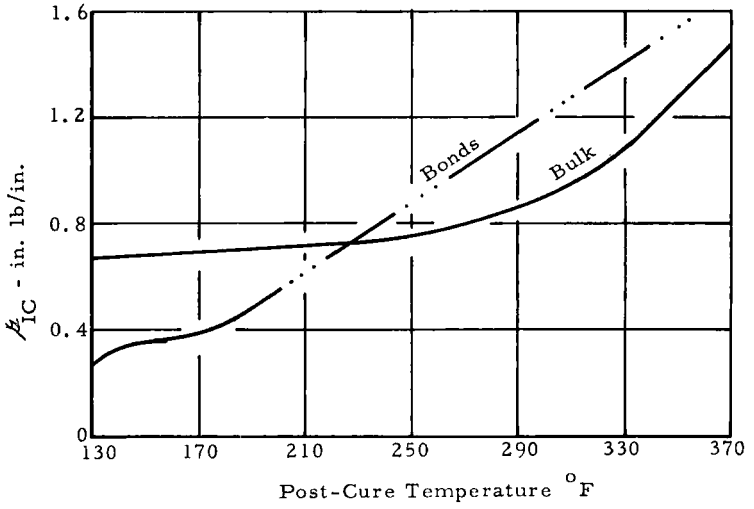

FIGURE 14 Toughness comparison of bulk and joints for 15 phr TEPA as a function of post-cure temperature. Post-cure time 5 hr.

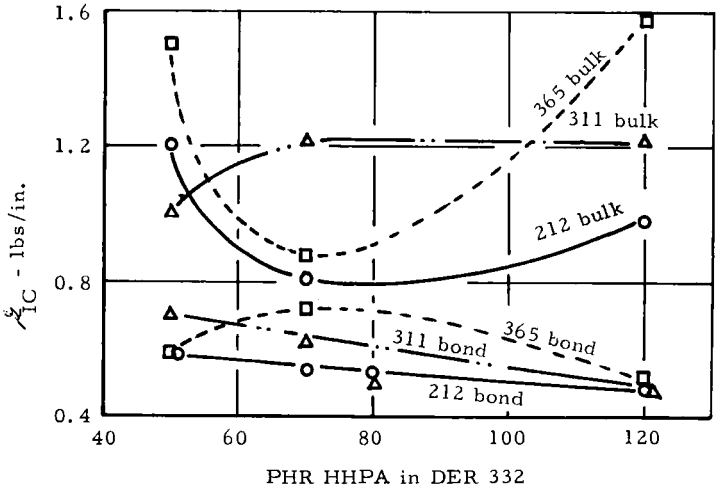

FIGURE 15 Toughness comparison between bulk and bond HHPA cured DER 332. Note bulk data lies above bond.

for both bulk and bonds, as hardener content and post-cure temperatures were increased. Nevertheless, the curves that relate these two manufacturing variables to toughness do depend on the differences in constraint that exist between the bulk resin and the same material used as an adhesive bond. A comparison plot of $\mathcal{G}_{IC}$ vs. post-cure temperature, Figure 14, indicates that bulk toughness may give either an under or over-estimate of bond performance.

Bulk and bond toughness data for the HHPA hardened resin was more disparate than that seen for the TEPA system, Figure 15. Bulk material was always tougher than bonds of the same make-up and, in some cases, the effects of the variables were to increase bulk performance, but decrease bond performance, or vice versa.

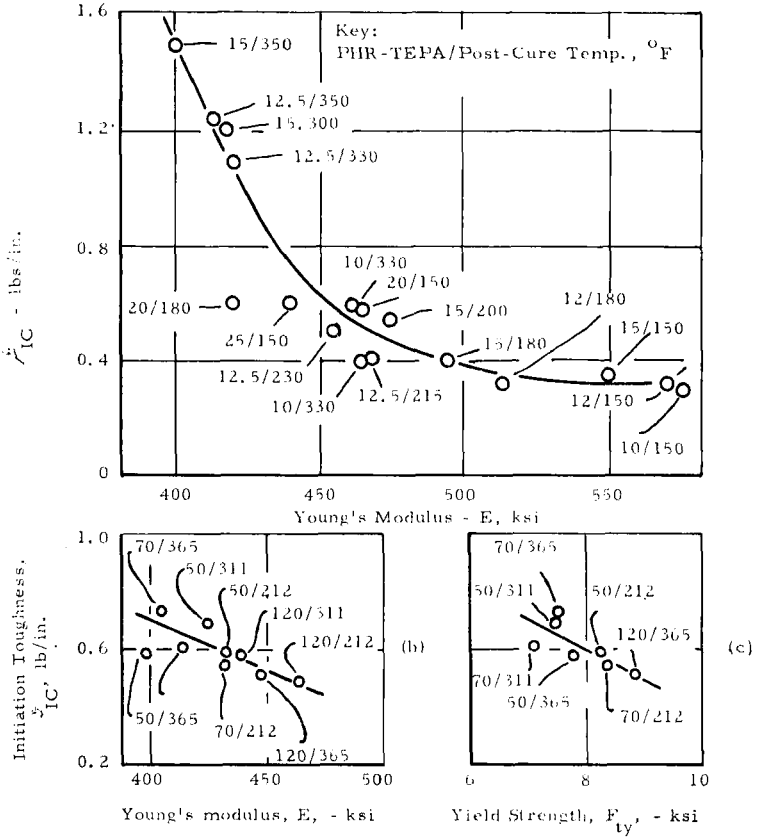

FIGURE 16 Dependence of joint toughness on (a) Young's modulus (TEPA cured DER 332), (b) Young's modulus (HHPA cured DER 332), and (c) yield strength at 1% total strain (HHPA cured DER 332). Refs. 4, 6.

RELATION OF SMOOTH TENSILE PROPERTIES TO BOND TOUGHNESS

Although bulk toughness does not predict bond toughness, within a given adhesive system, elastic modulus (or yield strength) is inversely related to joint toughness. This relationship, shown in Figure 16-a for TEPA cured resin, indicates that higher modulus is associated with lower toughness, irrespective of the composition and post-cure temperature that resulted in the high modulus. There is, however, little effect at all above modulus values of 500 ksi. A general trend of this sort, i.e., decreasing toughness for increasing modulus, was found with bulk epoxy toughness data, but no one-to-one correspondence was observed.

Bond toughness of HHPA cured resin showed decreased toughness with increased modulus or yield strength. Figure 16-b and c. The scatter and restricted range of moduli which are observed for the limits of hardener content and post-cure temperature studied do not obscure the same downward trend in toughness, although it is less pronounced than for TEPA cured resin.

CONCLUSIONS

1. For the two adhesive systems studied, rising-load bond toughness, $\mathcal{G}_{IC}$ cannot be predicted from the bulk toughness.
2. The large changes in bond toughness, i.e. 4:1 for TEPA cured resin, observed as hardener content and post-cure temperature are altered, is not predictable directly from tensile data.
3. Nevertheless, within a given epoxy system, the highest toughness will be obtained on material having the lowest modulus. Unfortunately, the different epoxies do not show the same value of toughness at a given value of E.
4. High cracking rates and large rate sensitivity are associated with a high $\mathcal{G}_{IC}$ value, i.e., initiation toughness appears to change over much broader limits than arrest toughness.
5. Within the range of practical interest, increases in bond thickness result in increased toughness.
6. The effect on toughness of changes in composition and post-cure temperature is much more pronounced in the room temperature amine (TEPA) cured resin than in the high temperature anhydride (HHPA) cured adhesive.
7. This difference in effect is not directly predictable from tensile property data, although the lesser change in tensile modulus or yield strength with changes in manufacturing variables for the HHPA system is consistent with lesser changes in toughness.

8. For those adherened materials that can be cleaned and treated in such a way that rising-load fracturing takes place in the center of the bond (CoB) rather than near one interface (IF), $\mathcal{G}_{IC}$ is independent of adherend material and surface finish.

Acknowledgements

This program was carried out under a series of contracts with the Naval Air Systems Command. The authors gratefully acknowledge their permission to publish this work. The many helpful suggestions of G. R. Irwin, Lehigh University, H. T. Corten, University of Illinois, and R. L. Patrick, Alpha R & D, are also gratefully acknowledged.

References

1. G. R. Irwin, "Fracture mechanics", in *Structural Mechanics* (Pergamon Press, 1960), pp. 557–594.
2. E. J. Ripling, S. Mostovoy, and R. L. Patrick, "Application of Fracture Mechanics to Adhesive Joints", STP No. 360, ASTM, 1963.
3. E. J. Ripling, S. Mostovoy and R. L. Patrick, *Mat. Res. and Stand.* **4,** 129 (1964).
4. S. Mostovoy and E. J. Ripling, *J. Appl. Poly. Sci.* **10,** 1351 (1966).
5. S. Mostovoy, P. B. Crosley, and E. J. Ripling, *Journal of Materials*, **2,** 661 (1967).
6. S. Mostovoy and E. J. Ripling, "Fracture Toughness and Stress Corrosion Cracking Characteristics of an Anhydride Hardened Epoxy Adhesive", Section I, Final Report, Contract No. N00019-69-C-0231.
7. S. Mostovoy and E. J. Ripling, "Effect of Joint Geometry on the Toughness of Epoxy Adhesives", Section II, Final Report, Contract No. N00019-69-C-0231.
8. E. J. Ripling, H. T. Corten and S. Mostovoy, this issue.
9. E. J. Ripling, C. Bersch and S. Mostovoy, this issue.